UNIAXIAL LOADING OF POLYMER-EMBEDDED GRAPHENE: IS ORTHOGONAL BUCKLING AVOIDABLE?

M.G. Pastore Carbone[1], G. Tsoukleri[1], I. Polyzos[1], J. Parthenios[1], K. Papagelis[1,2] and C. Galiotis[1,3]

[1]Foundation of Research and Technology Hellas, Institute of Chemical Engineering and High Temperature Processes, Stadiou St. Platani, GR-26504 Patras (Greece)
Email: mg.pastore@iceht.forth.gr, tsoukleri@iceht.forth.gr, ipolyzos@iceht.forth.gr, jparthen@iceht.forth.gr, c.galiotis@iceht.forth.gr, Web Page: http://graphene.forth.gr/
[2]Department of Materials Science, University of Patras, GR-26504 Patras (Greece)
Email: kpapag@upatras.gr, Web Page: http://www.matersci.upatras.gr/en/cv/299-papaggelis
[3]Department of Chemical Engineering, University of Patras, GR-26504 Patras (Greece)
Email: galiotis@upatras.gr, Web Page: http://www.chemeng.upatras.gr/en/personel/faculty/en/galiotis

Keywords: graphene, Raman spectroscopy, mechanical properties, orthogonal buckling, ribbon

Abstract
Graphene is believed to possess an extraordinary combination of mechanical properties in tension: high stiffnes, high strength and high ductility. However, due to several technical difficulties in the testing of atomically thin membranes, very little experimental verification has been provided for graphene's extraordinary mechanical properties. In particular, one of the critical aspect is the occurrence of lateral (orthogonal) buckling which may alter pure axial experiments. In order to prevent the occurrence of lateral buckling, we have altered the geometry of graphene flakes thus designing graphene micro-ribbons of specific dimensions which, when embedded to polymer matrices, can be stretched to at least moderate deformation without simultaneous buckling in the other direction. The design of micro-ribbons has been inspired by our previous findings about the critical strain to buckling of graphene flakes under compression and the minimum length which is needed to have sufficient stress transfer from the surrounding polymer matrix to the graphene. Graphene micro-ribbons have been thus fabricated by combining UV photolithography and dry etching oxygen plasma treatments onto CVD graphene. Finally, they were embedded into PMMA and, in order to investigate the mechanical response, the stress and strain along and across the micro-ribbons have been monitored by using Laser Raman Microscopy.

Excerpt from ISBN 978-3-00-053387-7

1. Introduction

Graphene is a perfect 2D crystal of covalently bonded carbon atoms that is a promising candidate in a number of electrical, thermal and mechanical applications, due to its exceptional physical properties [1,2]. Graphene also attracts great attention as strengthening component in composites, as it is attributed a unique combination of mechanical properties in tension [3]. However, in spite of graphene's potential as one of the stiffest and strongest material in nature, very little experimental verification has been provided for its extraordinary mechanical properties, owing to technical difficulties in the nanomechanical testing of atomically thin membranes. Among these, a significant critical aspect of axial mechanical measurements in tension is represented by instabilities phenomena leading to lateral (orthogonal) buckling which make pure axial experiments untenable. In fact, a thin film is expected to withstand relatively large tensile strains in air without early fracture, whereas in compression it is expected to buckle at low strains. Actually, graphene is estimated to buckle at extremely low strain ($\varepsilon_c \sim 10^{-9}$, according to molecular dynamics [4]); hence, for typical rectangular graphene flakes, it is obvious that, when the flake is stretched axially in one direction, Poisson's

contraction in the other direction will immediately induce lateral buckling making the performance of. pure axial experiements questionable. Recently, Polyzos et al. [5] have provided evidence that axial loading of graphene is always accompanied by the formation of orthogonal wrinkles similar to what is observed when a thin macroscopic membrane is stretched uniaxially. Also, the wrinkle formation was found to cause a variation of local axial strain between 0.05 to 0.22% (for a maximum applied strain of ~0.8%) which could induce premature failure at high strains. Very interestingly, for the system at hand, it was found that the buckling instability propagates into the portion of graphene which was embedded into the polymer grips.
Characterization of the mechanical properties of graphene is essential both from a fundamental interest in understanding its deformation physics and from a technological perspective for its reliable applications (e.g. as reinforcement in composites). In light of the above considerations, it emerges that, in order to gain reliable information on mechanical behavior of graphene, lateral buckling should be prevented in axial tensile deformation. Also, this represents the only possible route to exploit the full potential of graphene as an efficient reinforcement in composites.
In order to prevent lateral buckling, we have altered the geometry of the flakes thus tailoring graphene micro-ribbons of specific dimensions which, when embedded to polymer matrices, could be stretched to large deformation without simultaneous buckling in the other direction. The design of the micro-ribbons has been accurately performed taking into account some important experimental findings by our group [6-8]. Namely, under compression, the critical strain to buckling was found to be ~ -0.6% and independent of the flake's dimensions. Also, it was found that a minimum length of about 4 μm is needed in order to have sufficient stress transfer from the surrounding polymer matrix to the graphene [8]. Based on these findings, CVD graphene micro-ribbons were designed and produced by combining UV lithography and oxygen plasma. Finally, Raman mapping was adopted for detailed characterization of polymer-embedded micro-ribbons.

2. Material and Methods

2.1 Production of CVD graphene micro-ribbons

Graphene produced via CVD on 3-inch copper/silicon (Cu/Si) wafers was gently supplied by AIXTRON SE (Herzogenrath, Germany). Graphene micro-ribbons were produced directly on the Si/Cu wafer via UV standard lithography and oxygen plasma etching methods. The overall process for the production of graphene micro-ribbons and the transfer onto a polymer bar is schematized in Fig. 1. After the growth of graphene monolayer on a Cu/Si wafer (Fig. 1a), a thin layer (~1μm thickness) of a photoresist AZ 726MIF was spin coated on top at 5000 rpm for 30 sec and then was baked for 10min at 95oC (Fig.1b). Afterwards, the mask was loaded to the mask aligner and a positive UV standard lithographic process was performed for 7 sec (Fig. 1c), then the sample was developed in AZ 726MIF developer solution for 1min, rinsed with DI water and dried gently with nitrogen (Fig. 1d). Next, the wafer was placed in the etching chamber for 30 sec and, by following the below conditions: RF frequency = 13.56 MHz, RF power = 50 Watt, maximum vacuum = 10-4 mbar, pressure = 100 mTorr and oxygen N55 flow = 50 sccm, the uncovered graphene area was dry etched (Fig. 3e). Finally, acetone and 2-propanol were used to remove the remaining photoresist from the covered ribbons and the sample was rinsed with DI water and was dried gently with nitrogen (Fig. 1f).
The produced graphene micro-ribbons were embedded into a PMMA substrates by using the "wet transfer" method. According to this method, a thin transfer PMMA layer (~500nm thickness) of 495 K molecular weight dissolved in anisole (MicroChem) was first spin coated on top of the surface of the graphene micro-ribbons/Cu/Si wafer; then, the copper layer was etched in 1M solution of ammonium persulphate (APS). PMMA/graphene micro-ribbons membrane was floating on the solution and then was rinsed in DI water. Finally, the PMMA/graphene micro-ribbons thin film was "fished" by using a PMMA beam (Fig. 1h). During transfer process, care has been taken to align the micro-ribbons to the PMMA beam axis.

Excerpt from ISBN 978-3-00-053387-7

2.2 Characterization

Raman spectroscopy was used to evaluate the quality of the produced micro-ribbons. Raman spectra were recorded with the InVia Renishaw Raman system, under a 100x objective, by using an Argon ion laser (514.5 nm) and a diode laser (785 nm) as the excitation sources. Laser power on sample was kept below 0.25 mW in order to avoid laser-induced heating. A motorized xy stage allowthe collection of a large amount Raman spectra across the sample with a step size of 1 μm). By using the cantilever beam technique, uniaxial tensile and compressive loadings were applied to graphene micro-ribbons embedded into polymer substrates, collecting simultaneously Raman spectra in the middle of the ribbons. The beam was bended first in tension by steps of 0.1%, and then in compression by steps of 0.05%, by simply changing the bending direction. The polarization of the incident light was kept parallel to the applied strain axis. Detailed description of the apparatus and of sample geometry are reported elsewhere [6,7]. Atomic force microscopy (AFM) was carried out with a commercial AFM (Dimension icon, Bruker Co., USA) on micro-ribbons supported on PMMA films (i.e., before fishing procedure). The ScanAsyst mode was applied using silicon nitride tip (Scanasyst-Air, Bruker, nom. tip radius 2 nm, nom. frep. 70 kHz, nom. spring constant of 0.4 N/m) with scan resolution of 512 samples per line. Height mode images were acquired simultaneously at a fixed scan rate (0.1 Hz) with a resolution of 512 × 512 pixels.

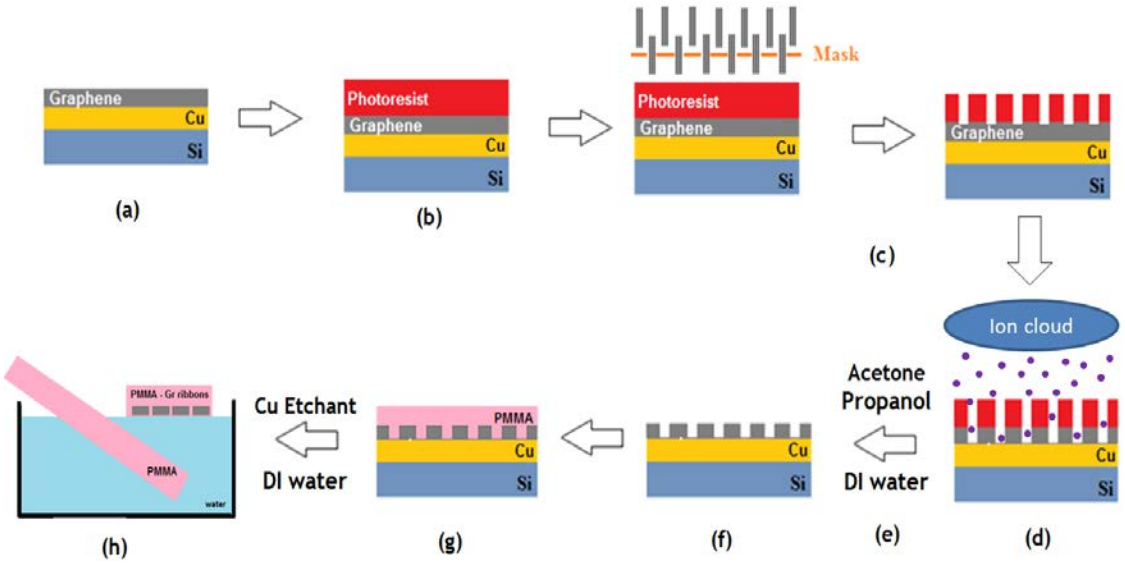

Figure 1. Fabrication of polymer-embedded CVD graphene micro-ribbons

3. Results and discussion

CVD graphene-microribbons. After photolithography/plasma process on the Gr/Cu/Si wafer, the fabricated graphene micro-ribbons are clearly observed under an optical microscope, due to the presence of the photoresist on top of them (Fig. 2a) and detailed Raman mappings were conducted using 514.5 nm excitation wavelength. A characteristic contour mapping is presented in Fig. 2b, where the blue areas correspond to produced graphene micro-ribbons of several widths from 1 to 4.5 μm. As can been seen, the contour is similar to the pattern of the designed basic unit, verifying that the above described production process was successfully performed.
After transferring on a PMMA bar, the effectiveness of the whole fabrication process and the quality of the embedded graphene micro-ribbon/PMMA samples have been investigated by using detailed Raman maps. The characteristic contour maps of frequency positions and of full width at half maximum (FWHM) of both G and 2D peaks are given in Fig. 3. The micro-ribbon appears well aligned to PMMA beam axis and shows a large distribution in the peak position and the FWHM of 2D

Excerpt from ISBN 978-3-00-053387-7

and G peaks, which points to a not perfectly flat micro-ribbon thus suggesting the presence of structural faults such as wrinkles, folds, substrate surface defects and molecular trapping induced by the fabrication and transferring process.

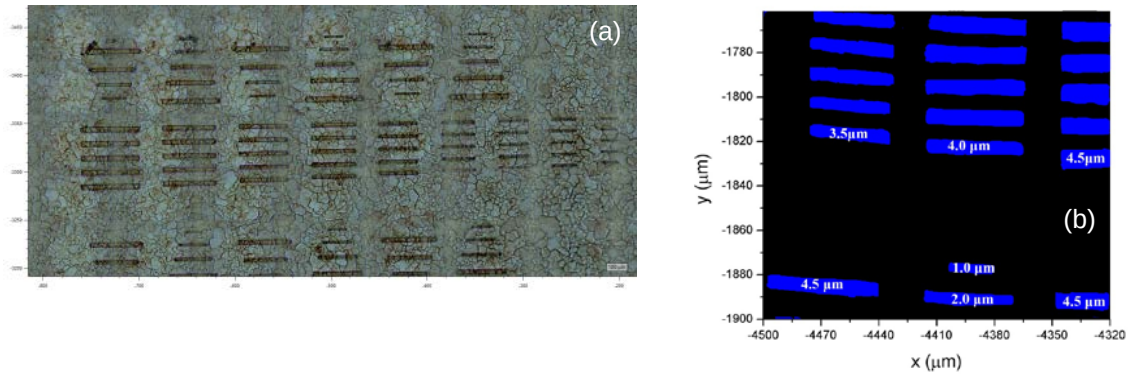

Figure 2. a) Optical image of produced graphene micro ribbons on Copper – Silicon wafer after Lithography and Plasma etching process. The micro – ribbons are still covered by the AZ 726MIF photoresist, b) Raman mapping on Graphene – Copper- Silicon wafer after dissolving AZ 726MIF photoresist

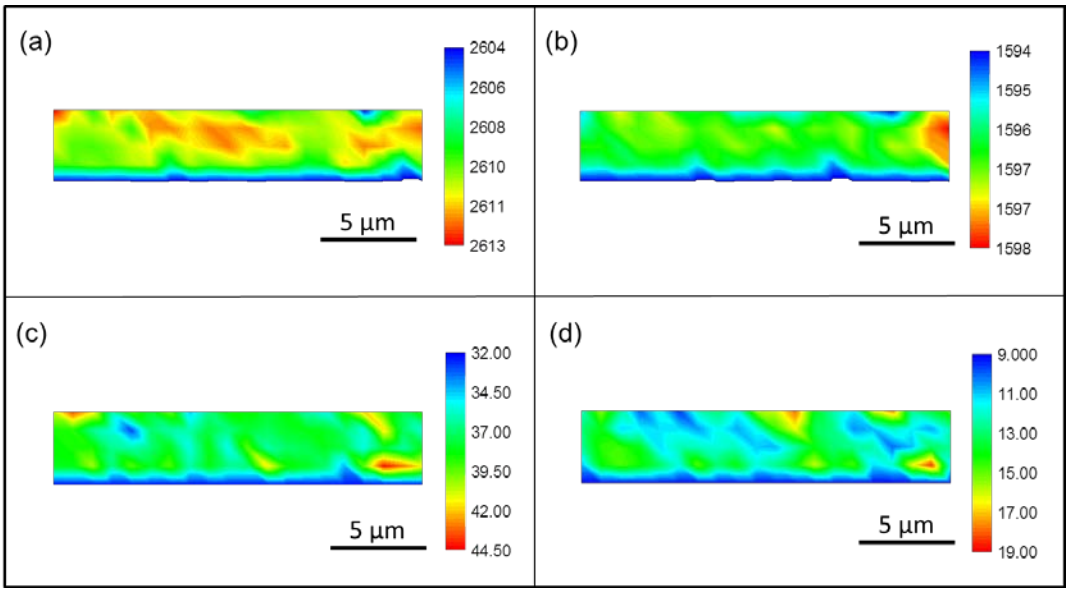

Figure 3. Characteristic contour maps of a) Pos(2D), b) Pos(G), c) FWHM(2D) and d) FWHM(G) of PMMA-embedded graphene micro-ribbon.

Table 1. Mean values and standard deviation of the position and FWHM of G and 2D bands for the PMMA-embedded microribbons.

	Pos(G) (cm^{-1})	*FWHM(G) (cm^{-1})*	*Pos(2D) (cm^{-1})*	*FWHM(2D) (cm^{-1})*
CVD	1596.2 ± 0.7	13 ± 2	2612 ± 1	38 ± 2

Excerpt from ISBN 978-3-00-053387-7

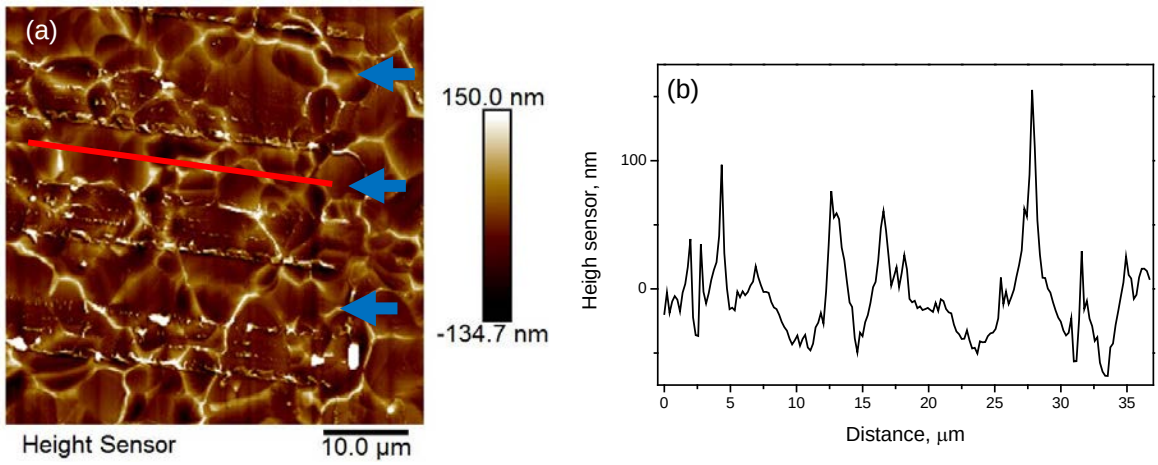

Figure 4. a) AFM image of a graphene micro-ribbons supported on PMMA and b) the corresponding height profile of the inset red line. Blue arrows indicate the micro-ribbons.

Statistical analysis of the maps has been performed and the mean values of positions and the FWHM of both 2D and G peaks are reported in Table 1. Based on the shift rates of the 2D and G Raman peaks for graphene flake under biaxial tensile deformations [9], the compressive strain experienced by the micro-ribbon can be estimated to be ~0.1 %. Furthermore, the average value of the ratio of the intensities of 2D and G peaks is ~0.7, likely suggesting chemical doping induced by the transfer process on the PMMA. Also, the corrugation of graphene micro-ribbons supported on PMMA has been verified by AFM (in Figure 4), revealing that the structure of graphene micro-ribbons is highly crumpled and that the polymeric substrate is not flat.

Representative Raman spectra in the G and 2D peaks spectral regions of graphene at several strain levels are shown in Figure 5, and the fitted positions of the G and of the 2D band as a function of strain are reported in Figure 6. In tension, it has been found that the positions of both 2D and G peaks show a linear behaviour with strain; the strain sensitivity (from the linear part of the graph, red lines) of 2D is -14.8 cm^{-1}/% ,while the strain sensitivity of G is -5.7 cm^{-1}/%. In compression, it has been found that the positions of both the 2D and G peaks exhibit a non-linear trend with strain. In particular, the average strain sensitivity in compression (from the linear part of the graph, red lines) of 2D is +12.3 cm^{-1}/%, while the strain sensitivity of G is +5.1 cm^{-1}/%. It should be noted here that G band splitting cannot be observed due to low deformation level experienced by the ribbons. The strain sensitivities found for CVD graphene micro-ribbons are much lower than those reported in literature for exfoliated graphene flakes. This has been already observed by Li et al.for CVD graphene on PET films[10]; in particular, the strain sensitivity of the 2D peak of a wrinkled CVD graphene was found to be less than 25% of the strain sensitivity of a flat exfoliated graphene flake. According to Li et al., the unusual Raman band shift behaviour observed is a result of the CVD graphene microstructure and was modelled in terms of mechanically isolated graphene islands separated by the graphene wrinkles. For the case at hand, apart from the wrinkled microstructure of CVD graphene arranged in islands, the adopted transfer procedure on a not perfectly flat substrate likely introduces further defects at the micro-ribbons/substrate interface (e.g., the aforementioned additional graphene corrugation, possible water and air trapping) thus reducing the efficiency of stress transfer.

Excerpt from ISBN 978-3-00-053387-7

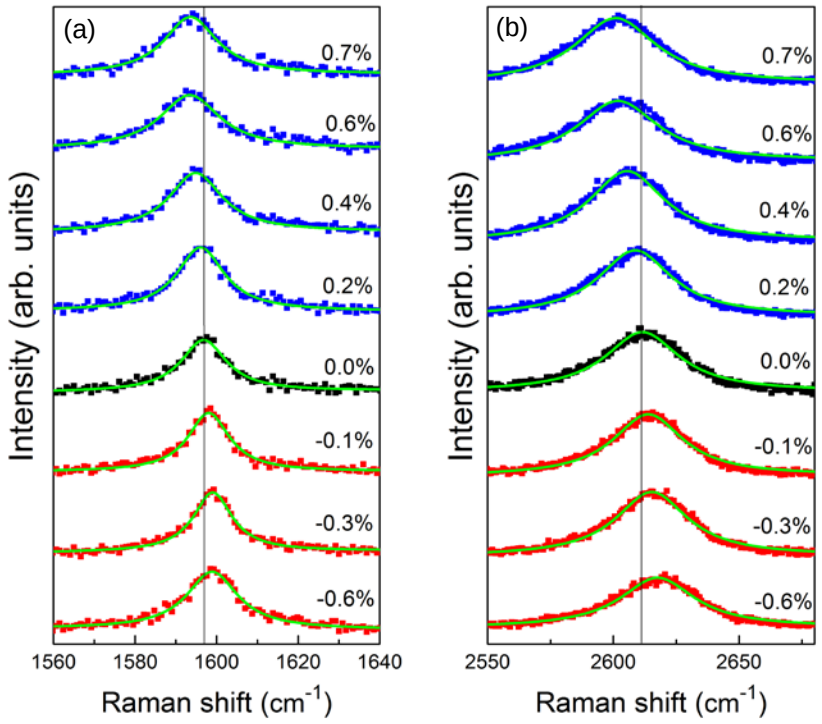

Figure 5. Evolution of the G (a) and 2D band (b) as a function of the strain, for the embedded CVD graphene micro–ribbons. The original measurements are plotted as points (blue for tension and red for compression).Solid lines represent Lorentzian fits to the experimental data.

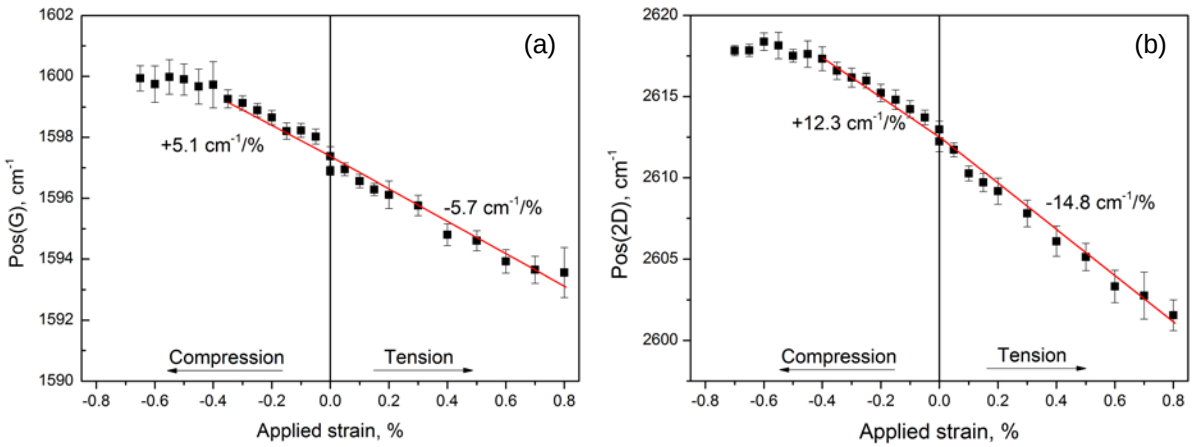

Figure 6. Position of G (a) and 2D (b) peak versus strain for the embedded CVD graphene micro–ribbons. Solid lines represent fits to the experimental data.

Excerpt from ISBN 978-3-00-053387-7

4. Conclusions

Avoiding lateral buckling is of paramount importance for the reliable characterization of the mechanical properties of graphene. It is also fundamental for the exploitation of the full potential of graphene as an efficient reinforcement in composites. For this reason, micro-ribbons of specific dimensions have been designed and produced from CVD graphene by combining UV lithography and oxygen plasma treatment. Detailed Raman mapping has proved the effectiveness of the proposed method and has evidenced that the embedded micro-ribbons show a large distribution in the peak positions and FWHM of the G and 2D bands most probably due to structural faults such as wrinkles, folds, substrate surface defects and molecular trapping induced by the fabrication and transferring process. Finally, the mechanical response of the PMMA-embedded micro-ribbons has been investigated by applying uniaxial tensile and compressive loadings to the sample, combined with the simultaneous collection of Raman spectra. Low values of strain rates of both 2D and G peaks have been found thus suggesting inefficient stress transfer through the graphene micro-ribbons/polymer interface, likely due the aforementioned structural faults. Unfortunately, the highly crumpled configuration has hindered the detailed investigation of the stress-strain characteristics of the embedded micro-ribbons and thus the eventual suppression of lateral buckling. Attempts to refine the transfer method (also combined with an ad-hoc procedure for ironing out graphene wrinkles) for appropriate mechanical investigation are in progress.

Acknowledgments

This research has been co-financed by the European Research Council (ERC Advanced Grant 2013) via project no. 321124, ‘‘Tailor Graphene’’. Finally, the authors acknowledge the financial support of the Graphene FET Flagship (‘‘Graphene-Based Revolutions in ICT And Beyond’’— Grant Agreement No: 604391).

References

[1] A. K. Geim and K. S. Novoselov. The Rise of Gaphene. *Nature Materials* 6:183-191, 2007
[2] K. S. Novoselov, Graphene: Materials in the Flatland. *Reviews of Modern Physics* 83, p. 837-49, 2011.
[3] C. Lee, X. Wei, J. W. Kysar, and J. Hone. Measurement of the Elastic Properties and Intrinsic Strength of Monolayer Graphene. *Science* 321: 385-388, 2008.
[4] Y. Gao, P. Hao. Mechanical Properties of Monolayer Graphene under Tensile and Compressive Loading. *Phys. E* 41:1561–1566, 2009.
[5] I. Polyzos, M. Bianchi, L. Rizzi, E. N. Koukaras, J. Parthenios, K. Papagelis, R. Sordan and C.Galiotis. Suspended monolayer graphene under true uniaxial deformation. *Nanoscale*, 7:13033-13042, 2015.
[6] O. Frank, G. Tsoukleri, J. Parthenios, K. Papagelis, I. Riaz, R. Jalil, K. Novoselov, and C. Galiotis. Compression Behavior of Single-Layer Graphenes, *ACS Nano* 4: 3131-3138, 2010.
[7] G. Tsoukleri, J. Parthenios, K. Papagelis, R. Jalil, A. C. Ferrari, A. K. Geim, K. S. Novoselov, and C. Galiotis. Subjecting a Graphene Monolayer to Tension and Compression. *Small* 5: 2397-2402, 2009.
[8] C. Androulidakis, E. N. Koukaras, O. Frank, G. Tsoukleri, D. Sfyris, J. Parthenios, N. Pugno, K. Papagelis, K. S. Novoselov, and C. Galiotis. Failure Processes in Embedded Monolayer Graphene under Axial Compression. *Sci. Rep.* 4: 5271, 2014.
[9] C. Androulidakis, E. N. Koukaras, J. Parthenios, G. Kalosakas, K Papaggelis and C. Galiotis. Graphene flakes under controlled biaxial deformation. Sci. Rep. 5: 18219, 2015.
[10] Z. Li, I. A. Kinloch, R. J. Young, K. S. Novoselov, G. Anagnostopoulos, J. Parthenios, C. Galiotis, K. Papagelis, C.-Y. Lu, L. Britnell. Deformation of Wrinkled Graphene, *ACS Nano* 9;3917–3925, 2015.

Excerpt from ISBN 978-3-00-053387-7